

This is the peer reviewed version of the following article: Cai, W, Liu, J, Liu, P, et al. A direct carbon solid oxide fuel cell fueled with char from wheat straw. Int J Energy Res. 2019; 43(7): 2468–2477, which has been published in final form at <https://doi.org/10.1002/er.3968>. This article may be used for non-commercial purposes in accordance with Wiley Terms and Conditions for Use of Self-Archived Versions. This article may not be enhanced, enriched or otherwise transformed into a derivative work, without express permission from Wiley or by statutory rights under applicable legislation. Copyright notices must not be removed, obscured or modified. The article must be linked to Wiley's version of record on Wiley Online Library and any embedding, framing or otherwise making available the article or pages thereof by third parties from platforms, services and websites other than Wiley Online Library must be prohibited.

A direct carbon solid oxide fuel cell fueled with char from wheat straw

Weizi Cai^{1,2}, Jiang Liu^{1,*}, †, Peipei Liu¹, Zhijun Liu¹, Haoran Xu², Bin Chen²,

Yuzhi Li¹, Qian Zhou¹, Meilin Liu^{1,3}, Meng Ni^{2,*}, †

¹ Guangzhou Key Laboratory for Surface Chemistry of Energy Materials, New

Energy Research Institute, School of Environment and Energy, South China

University of Technology, Guangzhou 510006, P. R. China.

² Building Energy Research Group, Department of Building and Real Estate, The

Hong Kong Polytechnic University, Hung Hom, Kowloon, Hong Kong 999077, P. R.

China.

³ School of Materials Science and Engineering, Georgia Institute of Technology,

771Ferst Drive, Atlanta, GA 30332-0245, USA.

Correspondence

*Jiang Liu, Guangzhou Key Laboratory for Surface Chemistry of Energy Materials,

New Energy Research Institute, School of Environment and Energy, South China

University of Technology, Guangzhou 510006, P. R. China.

†E-mail: jiangliu@scut.edu.cn

*Meng Ni, Building Energy Research Group, Department of Building and Real Estate,

The Hong Kong Polytechnic University, Hung Hom, Kowloon, Hong Kong 999077, P.

R. China.

†E-mail: bsmengni@polyu.edu.hk

SUMMARY

Direct carbon solid oxide fuel cell (DC-SOFC) is a promising technology for electricity generation from biomass with high conversion efficiency and low pollution. Biochar derived from wheat straw is utilized as the fuel of a DC-SOFC, with cermet of silver and gadolinium doped ceria (Ag-GDC) as the material of both cathode and anode and yttrium stabilized zirconia (YSZ) as electrolyte. The output performance of a DC-SOFC operated on pure wheat straw is 197 mW cm^{-2} at 800°C , and increases to 258 mW cm^{-2} when 5 % of Ca, as a catalyst of the Boudouard reaction, is loaded on the wheat straw char. Higher power and fuel conversion utilization are achieved using Ca as the Boudouard reaction catalyst. X-ray diffraction (XRD), scanning electron microscopy (SEM), energy dispersive spectrometer (EDX) and programmed-temperature gravimetric experiment are applied to characterize the leaf char. It turns out that the wheat straw char is with porous structure and composed of C, K, Mg, Cl, Fe and Ca elements. The effects of the Ca catalyst on the Boudouard reaction, the performance of the DC-SOFCs operated on the wheat straw char and the economic advantages of the wheat straw char are demonstrated and analyzed in detail.

Key words

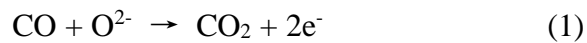
Solid oxide fuel cells; carbon fuel; direct carbon fuel cell; Boudouard reaction; biochar

1. INTRODUCTION

Energy demand is an eternal topic for human beings because of growing energy price, resource depletion and environmental pollution. Currently, fossil fuel is still the major energy source in the world, contributing to 80 % of the global primary energy supply [1]. Biomass, an important carbon-neutral renewable energy resource, can directly convert solar energy to chemical energy through photosynthesis, implying that biomass is a green energy carrier. Actually, the world energy demand reaches 5.67×10^{20} J in 2013, while the bioenergy captured by land plants is 3–4 times greater than human energy demands [2]. Wheat straw is an agricultural byproduct, which is available in plentiful amount in all over the world. The average yield of wheat straw is about 1.4 kg kg⁻¹ of wheat grain [3]. Only in China, over 700 million tons of wheat straw are produced in 2015. Although, wheat straw is a biomass resource with low energy density, which causes the cost of collection to be the main part of the wheat straw, the price of the wheat straw is as low as 150 CNY ton⁻¹ [4]. In rural areas of China, there is substantial biomass resources, but insufficient electricity supply. It is particularly suitable to directly convert the enormous amount of local biomass resources to electricity in such rural areas in developing countries. Conventionally, combustion is the main way to apply the energy stored in wheat straw, whose energy conversion efficiency is low [5]. Moreover, noxious gases, such as CO, SO₂ and NO_x, are formed and emitted, resulting in serious air pollution [6]. Therefore, alternative ways to convert the biomass energy cleanly and efficiently are in great need. What's more, low cost and wide distribution of biomass resources and emergency needs of power supply provide development space and unique

advantages for novel energy conversion technologies.

Direct carbon solid oxide fuel cell (DC-SOFC) has been regarded as one of the most promising power generation technologies that can continuously convert solid carbon into electrical energy with high thermodynamic conversion efficiency and low pollution as long as the carbon fuel is supplied [7-15]. As early as 1988, Nakagawa and Ishida first studied a direct carbon solid oxide fuel cell (DC-SOFC) without any liquid material [16]. From their experimental results, they proposed the mechanism of DC-SOFC, which consisted of electrochemical reaction of CO (1) and carbon gasification reaction, known as Boudouard reaction (2):



By comparing the performances and the impedance spectra of a SOFC operated respectively on activated carbon and dry CO, Xie et.al. have verified the reaction mechanism [17]. During the discharging process, CO in the anode chamber takes electrochemistry reaction with oxygen anions O^{2-} on the anode to perform reaction (1) and donate electrons to the external circuit. As the reaction product of reaction (1), CO_2 would diffuse to and react with the solid carbon to produce more CO (2). In this way, C is continuously delivered from the solid carbon to the anode to maintain the electrochemical reaction for generating electricity [18, 19]. In other words, CO and CO_2 are vehicles for delivering solid carbon fuel to the DC-SOFC. Therefore, there is not any necessary for carbon particles to have a physical or chemical contact with the anode

of the cell, which is the most significant difference and advantage to other kinds of direct carbon fuel cells (DCFCs) [20]. Accordingly, catalyzing both of reactions (1) and (2) is a simple and effective way to improve the DC-SOFC performance. Tang et al. applied silver-gadolinium doped ceria (GDC, $\text{Gd}_{0.2}\text{Ce}_{0.8}\text{O}_{1.9}$) as anode materials to catalyze the electro-oxidation of CO and Fe on activated carbon to catalyze the carbon gasification reaction, which significantly improve the cell performance from 4 to 46 mW cm^{-2} at 800 °C [21]. Later on, a Ni-YSZ anode-supported SOFC stack fueled by Fe-loaded activated carbon was developed and yielded a peak power density of 465 mW cm^{-2} at 850 °C [22].

Different kinds of biomass-derived fuels have been applied in direct carbon fuel cells to generate electricity [12, 23-25]. Almond shell biochar and coconut biochar are utilized to generate electricity in SOFCs by Elleuch et al. and relatively high performances of 127 mW cm^{-2} and 105 mW cm^{-2} at 700 °C are achieved respectively [23]. Recently, bioethanol and glycerol have been used as fuel in low-temperature solid oxide fuel cells by Zhu [26]. A maximum power density of 215 mW cm^{-2} was observed by using glycerol as fuel at 580 °C. However, an extra pyrolysis system was demanded to thermal decompose and steam glycerol and bioethanol which increases the system complexity. A DC-SOFC powered by a plant derived biofuel with natural catalyst was studied by Liu et al. [18]. The maximum power density of the DC-SOFC was 212 mW cm^{-2} at 850 °C, even slightly higher than that operated on Fe-loaded activated carbon (201 mW cm^{-2}). It can be seen from above, SOFC is a promising technology for

recycling use of agriculture byproduct.

In this paper, in order to provide initial guidance for policymakers, we report our work on using wheat straw char as the fuel of all-solid-state DC-SOFCs to achieve the goal of efficient reuse of agriculture byproduct. The property and structure of the wheat straw char are examined. The impedance spectra, discharging characteristics and fuel utilization of the corresponding DC-SOFCs are tested and analyzed in detail.

2. EXPERIMENTAL

2.1. Pre-treatment of carbon fuels

One year old wheat straw was collected as agriculture byproduct from local farmland in Zhengzhou city, Henan province of China (34°38'N 112°57'E). Wheat straw was dried at 150 °C in an oven for overnight, following by heating in a tubular furnace at 700 °C for 2 hours without any carry gases. The tubular furnace was sealed up, except a gas conductive pipe to allow the produced gases outside from the furnace. Then, it was pulverized into powder and sieved through a 150 mesh sieve. An infiltration process is used to load Ca on the wheat straw char. Firstly, to prepare 10 g of Ca-loaded wheat straw char (5 wt. % of Ca), 2.98 g of $\text{Ca}(\text{NO}_3)_2 \cdot 4\text{H}_2\text{O}$ was dissolved in deionized water under stirring. Secondly, under stirring, 9.5 g of wheat straw char was added into the $\text{Ca}(\text{NO}_3)_2$ solutions. After stirring for 1 hour, the turbid solution was heated at 80 °C till it was dried. Then, the catalyst-loaded carbon fuel was transferred to a tubing oven, followed by heating at 400 °C for 1 h under N_2 atmosphere. After heat-treatment,

$\text{Ca}(\text{NO}_3)_2$ would decompose and deposit on the surface of wheat straw. The content of the loading Ca element is 5 wt. %, which is the optimal loading content for catalyst-loaded carbon fuels of DC-SOFCs. The detail experiment process and mechanism have been reported in our previous work [27].

2.2. Fabrication of SOFCs

Button cells with a configuration of Ag-GDC/ YSZ/ Ag-GDC were fabricated in steps described as following: Firstly, an electrolyte support of yttria-stabilized zirconia (8YSZ, Tosoh Corporation, Japan) was fabricated by dry pressing method (0.05 g in weight and 13 mm in diameter), followed by sintering at 1400 °C in air for 4 h [28] . A dense YSZ electrolyte wafer with a thickness of 0.2 mm and diameter of 11 mm was obtained. Secondly, silver paste (DAD-87, Shanghai Research Institute of Synthetic Resins, Shanghai, China) and GDC powder (purity $\geq 99.5\%$, particle size: $d_{50}=0.5\sim 3\ \mu\text{m}$, Ningbo Institute of Materials Technology and Engineering, China) were ground in an agate mortar for 3 h to get an uniform Ag-GDC slurry (weight ratio of 70:30). Then the slurry was painted on both sides of the electrolyte pellets followed by firing at 850 °C for 4 h. Through a mask with a hole in the middle, the cathode area was controlled to be $0.28\ \text{cm}^2$. Thirdly, a silver paste was used to paint silver grids, as current collector, on the anode and cathode, respectively. Ag-GDC was chosen as anode and cathode material for the DC-SOFCs, because of the excellent electronic conductivity and stability of Ag, the high O^{2-} conductivity and CO oxidation catalytic effect of GDC, and

simplification of the fabricating process [19, 21].

2.3. Cell assembling and characterization

As sealing and jointing materials, silver paste was applied to connect the cells to one end of an alumina tube. Silver wires were attached to the electrodes, and connected to an Iviumstate electrochemical analyzer (Ivium Technologies B.V., Netherlands). An SOFC fueled by humidified hydrogen (volume fraction of H₂O: 3%) was first tested to evaluate the typical as-prepared cells. The hydrogen gas flow rate was 30 cm³ min⁻¹. For the DC-SOFCs, 0.4 g of carbon fuel was filled into each cell. A rubber stopper with an airway pipe was used to block on the other end of the alumina tube, and leading the emitted gas out. In all testing experiments, the cathode side of DC-SOFC was exposed to ambient air (Figure 1). The alternating current voltage perturbation applied in the impedance measurement of the cells is 10 mV, with a frequency range of 0.1- 10⁵ Hz. The morphology and composition of the SOFCs and the carbon fuel were characterized by a scanning electron microscope (SEM, Carl Zeiss AG-Merlin, Germany). The carbon gasification reactivity of all the catalyst-loaded carbon fuels is investigated under programmed-temperature conditions using a Thermogravimetric analyzer (TGA, Mettler Toledo, Switzerland). In each gasification experiment, 9-10 mg of carbon fuel was loaded in ceramic pan under a flowing N₂ atmosphere with a flow rate of 50 cm³ min⁻¹ and a heating rate of 20 °C min⁻¹ from 25 °C to 800 °C. After the temperature reached 800 °C, the atmosphere was switched to CO₂ (50 cm³ min⁻¹). X-ray diffraction

(XRD, Rigaku D/max-III A diffractometer, Japan, Cu-K α radiation, operated at 35 kV, 30 mA, $\lambda = 1.54184 \text{ \AA}$) was performed on the carbon fuel before discharging process. The Raman spectra of carbon fuels were performed using a LabRAM HR800 spectrometer (Horiba Jobin Yvon, FR.) with a wavelength of 532 nm.

Figure 1. Schematic illustration of a direct carbon solid oxide fuel cell.

3. RESULT AND DISCUSSION

3.1. Characteristics of the as-prepared SOFCs

Figure 2. SEM pictures of anode (a) and electrolyte (b) of the as prepared SOFC.

Figure 2 shows the microstructures of the as prepared SOFCs. From Figure 2(a), we can find that the thickness of the anode layer is about $21 \mu\text{m}$, which closely attaches to the YSZ electrolyte. The anode is fairly porous with relatively uniform microstructure. Figure 2(b) reveals that the YSZ electrolyte is fairly dense, only with a few of closed pores which would not affect the gas tightness of the DC-SOFCs.

Figure 3. Output performances (a) and impedance spectra (b) of the as-prepared

SOFC operated on humidified hydrogen at 800 °C.

Figure 3 is the output performances and impedance spectra of the as-prepared SOFC operated on humidified hydrogen at 800 °C. As shown in Figure 3(a), an open circuit voltage (OCV) of 1.04 V is achieved, indicating that the YSZ electrolyte is dense and the SOFC is well sealed. A maximum power density of 301 mW cm⁻² is obtained, which is reasonable for an electrolyte-supported SOFC, indicating that the SOFCs are commendably prepared. The cell ohmic resistance is about 0.44 Ω cm², which can be read from the intercept of the real axis at high-frequency on the impedance spectrum (Figure 3b). Meanwhile, the difference between the overall resistance and the ohmic resistance, which is corresponding to the polarization resistance of the cell, is about 0.39 Ω cm².

3.2. Characterizations of carbon fuels

Figure 4. SEM micrographs (a, b) and EDX results (c) of wheat straw char.

The SEM images and EDX result of the wheat straw char are shown in Figure 4. It can be seen that the average size of wheat straw char is around 100 μm (Figure 4a). What's more, Figure 4(b) shows that the surface of the wheat straw char is fairly rough, which has many large pores with irregular carbon walls. The energy dispersive

spectrometer (EDX) results shows that, beside the dominant content of carbon, Si along with some K, Mg, Cl, Fe and Ca are detected on the wheat straw char. In addition, the content of oxygen, with an atom fraction of 28.65 %, is relatively high. It indicates that the as-mentioned metal elements might mainly exist in the form of metal oxides or carbonates. Noted that K, Mg, Fe element also are excellent Boudouard reaction catalysts [29]. The elements may be beneficial to the cell performance of a DC-SOFC operated on wheat straw char as fuel. However, there is also 7.01 % of silicon existed on the wheat straw char. As we all know, silicon is a toxicant for SOFC, especially for a Ni-YSZ anode-support SOFC. Fortunately, there is not any direct contact between wheat straw char and the anode of the cell, so the silicon existing on the wheat straw char might not affect the performance of the DC-SOFC.

Figure 5. X-ray diffraction spectra for pure wheat straw char and Ca-loaded wheat straw char.

To determine the composition of the wheat straw char, an X-ray diffraction is measured, as shown in Figure 5. Apparently, before loading Ca on the wheat straw char, there is a cubic system of KCl, indicating that KCl is one of the main components of the wheat straw char. It confirms the existence of K and Cl elements as detected by the EDX analysis. After loading Ca on the wheat straw char, two peaks, respectively situate at 28° and 30° , are attributed to CaCO_3 . It is clearly shown that Ca is loaded on the

wheat straw char in the form of CaCO_3 . For another, two broaden peaks, locating around 2θ values of 25° and 44° , are attributed to the reflection of (002) and (100) crystal faces of graphite and amorphous carbon. It is well known that diffraction peaks become broad with the decrease of crystal size. Therefore, it can be supposed that the wheat straw char is composed of graphite and amorphous carbon with small grain size. In fact, the crystallization of carbon significantly affects the number of carbon gasification reaction active sites. In other words, carbon atoms in the form of amorphous carbon are more reactive than that as graphite.

Figure 6. Raman spectra of wheat straw and commercial graphite.

Rama spectroscopy is also applied to characterizing the graphitic structure of wheat straw, as shown in Figure 6. As comparison, the Rama spectra of commercial graphite is also shown in the figure. It has been demonstrated that the G band of the first-order Rama spectra of carbons is attributed to the sp^2 carbon atoms in the graphitic lattice, while the D band corresponds to the vibrations of carbon atoms in the disordered carbon. The peak intensity ratios of the D band G band is strongly related to the graphite carbon content of the sample. Figure 6 shows that the relative intensity of D band to G band (I_D/I_G) for the wheat straw char is significantly larger than that for the commercial graphite. What's more, the I_D/I_G value of wheat straw char is about 1:1, demonstrating

the existence of large amount of disorder carbon in the wheat straw char, which might promote the carbon gasification reaction activity.

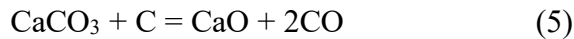
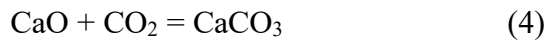
Figure 7. Carbon conversion of pure wheat straw char and Ca-loaded wheat straw char under CO₂ atmosphere at 800 °C.

For the carbon gasification reaction ($\text{CO}_2 + \text{C} \rightarrow 2\text{CO}$), it has been widely recognized that calcium oxide and calcium carbonate are excellent catalysts with reasonable catalytic effect and low cost [30, 31], and its catalyzing mechanisms on different operating conditions have been well studied [32-35]. However, to further demonstrate the catalytic activity of Ca on the wheat straw char, a programmed-temperature gravimetric experiment is conducted on the pure wheat straw char and the Ca-loaded wheat straw char. Carbon conversion (x) is calculated through the following formula:

$$x = \frac{w_0 - w_t}{w_0 - w_r} \quad (3)$$

where w_t is the mass at gasification time t , w_0 is the origin mass of the char at the beginning of gasification, and w_r is the mass of ash and catalyst remaining after gasification experiment. The carbon conversions of carbon fuels with and without Ca catalyst are showed in Figure 7. In our TGA experiment, the thermogravimetric analyzer records a data point each 0.5 second automatically, meaning that there are

about 6000 data points for a carbon conversion curve. Therefore, the carbon conversion curves shown in Figure 7 are relatively smooth. Obviously, the carbon conversion rate of pure wheat straw char is obviously lower than that of Ca-loaded one, indicating that the gasification reactivity of wheat straw char increases because of the Ca catalyst. Therefore, Ca is loaded on the wheat straw char as a fuel for DC-SOFCs to promote the Boudouard reaction for producing sufficient carbon monoxide to the electrochemistry reaction of the anode. Actually, a “spill-over” model can be used to described the mechanism of metal catalytic carbon gasification [33]. Specifically, First of all, CO₂ adsorbs and dissociates on a metal catalyst and forms a metal catalyst-CO₂ complex. Secondly, the metal catalyst-CO₂ complex transfers to nearby carbon substrate to take reaction with a carbon atom, producing two CO molecules. For the Ca catalyzed carbon gasification, CaO is highly active on chemisorption of CO₂ and further to form CaCO₃, followed by the solid-state reaction between CaCO₃ and carbon. The mechanism is described as the following model [36]:



In this model, the reaction rate-determining step is reaction (5). In fact, a catalyst particle must solubilize it at the interface to react with the carbon substrate. To solubilize carbon atoms, a catalyst particle must has active contact with carbon atoms. To have active contact, there must be a so-called “sintering-like” faceting of the catalyst particle [29]. Accordingly, Tammann temperature, at which lattices begin to be

appreciably mobile, is applied to evaluate the catalytic activity of a metal oxide on the carbon gasification reaction. Actually, the Tammann temperatures of CaCO_3 is as low as 533 K. Benefited from a low Tammann temperature, at the cell operation temperature of 1073 K, Ca exhibits such good catalytic properties for the carbon gasification reaction (Boudouard reaction).

3.3. Electrochemical performance of DC-SOFCs

Figure 8. Output performances (a) and impedance spectra at OCV (b) of the DC-SOFCs operated at 800 °C, respectively with pure wheat straw char and Ca-loaded wheat char as fuel.

Figure 8(a) shows the electrochemical performance of two DC-SOFCs operated at 800 °C, respectively using pure and Ca-loaded wheat straw char as fuel. The OCVs for both cells are about 0.98 V, comparable to a theoretical OCV of DC-SOFC at 800 °C, 1.04 V. The peak power density of the DC-SOFC with pure wheat straw char is 197 mW cm^{-2} . When Ca catalyst is loaded on the char, the peak power density increases to 258 mW cm^{-2} , indicating that Ca exhibits good catalytic effect for Boudouard reaction. Figure 8(b) reveals the electrochemical impedance spectra of the DC-SOFCs measured under open circuit voltage. The ohmic resistances of the cells are

almost the same ($0.43 \Omega \text{ cm}^2$) due to the identical operating temperature and SOFC configuration. However, the polarization resistances of the cells are not the same. The electrode polarization resistance is approximately $0.48 \Omega \text{ cm}^2$ for the cell with Ca-loaded wheat straw char and $0.62 \Omega \text{ cm}^2$ for the cell without Ca catalyst. It is understandable that a pure wheat straw char DC-SOFC reveals a higher polarization resistance, since the carbon gasification reaction (2) rate is not fast enough to produce sufficient CO for the electrochemical reaction (1). The better output performance and lower polarization resistance of the DC-SOFC powered by Ca-loaded wheat straw char than those of the pure wheat straw char DC-SOFC suggests that the Boudouard reaction within the Ca-loaded wheat straw char DC-SOFC is better catalyzed than that within the other.

Figure 9. Discharging characteristics of DC-SOFCs respectively with 0.4 g pure wheat straw char and Ca-loaded wheat straw char, operated at constant current of 300 mA cm^{-2} , at 800°C .

Figure 9 are the discharging curves of the DC-SOFCs, respectively with 0.4 g pure wheat straw char and Ca-loaded wheat straw char, operated at a constant current of 300 mA cm^{-2} at 800°C . Both of the cells continuously discharge at a relatively smooth platform, and abruptly drop to 0 V. Although same quality of carbon fuels are filled into

the DC-SOFCs, the two cells reveal totally different discharging time and discharging voltage. The discharging time of the cell powered by Ca-loaded wheat straw char is about 10.2 h, with a discharging plateau (0.68 V) markedly higher than that of pure wheat straw char cell (0.60 V, 4.8 h). Higher discharging voltage and longer discharging time indicate that the former cell offers higher power and fuel conversion efficiency. For the cell with Ca-loaded wheat straw char, the total discharging time is about 10.2 h, at a discharging current of 85 mA. During the discharging process of the cell, there is 3121 C charge delivered, indicating that 0.097 g of carbon has been consumed through electrochemical reaction, taking the overall reaction of the DC-SOFC as 4-electrons reaction ($C + 2O^{2-} \rightarrow CO_2 + 4e^-$). From the TG experiment, we find that there is about 27% of minerals (weight percent) in the Ca-loaded wheat straw char, which leads to 73% of carbon (weight percent) in the carbon fuel. Therefore, the carbon fuel utilization of the Ca-loaded wheat straw char cell is 33.3 %, as 0.4 g carbon fuel has been filled into the DC-SOFC. Similarly, the carbon fuel utilization of the pure wheat straw char cell would be 15.7 %, which is much lower than that of the Ca-loaded carbon fuel cell. This is a further indication of the positive effect of Ca catalyst to the carbon gasification reaction and the superiority of the Ca-loaded wheat straw in preparing carbon fuel for DC-SOFCs.

Figure 10. Microstructures of the Ca-loaded wheat straw char before (a) and after

(b) cell discharging operation.

After discharging for 10.2 h, the cell is cool down to room temperature and the remainder of Ca-loaded wheat straw char is collected to measure the microstructures through SEM technique. For comparison, a SEM picture of the Ca-loaded wheat char before discharging test is also provided in Figure 10(a). As shown in Figure 10(b), the Ca-loaded wheat straw char powders are sintered into larger agglomerates with particle size of 20-300 μm , which is significantly larger than that before operation (Figure 10a). Moreover, the particles of the Ca-loaded wheat straw char after operation are dense, comparing that before operation, which demonstrates that the decline of the DC-SOFC is caused by consumption and sintering of the carbon fuel.

Table 1. Comparison of different carbon fuels applied on DC-SOFCs.

Carbon fuel	Price of carbon fuel (CNY t^{-1})	Catalyst	Cell configuration	MPD of DC-SOFC (mW cm^{-2})	Temperature ($^{\circ}\text{C}$)
Wheat straw char (the work)	150	Ca	Ag-GDC/ YSZ/ Ag-GDC	258	800
Activated carbon [22]	6000	Fe	Ni-YSZ/ YSZ/ LSM	465	850
Graphite [21]	2500	None	Ag/ YSZ/ Ag	9.3	800
Ash-free coal [37]	500-800	None	Ni-YSZ/ YSZ/ LSM-GDC /LSM	90	840

Table 1 is a comparison of different carbon fuels applied in DC-SOFCs. As we can see, the price of the wheat straw is only 2.5 % of that of activated carbon, and

significantly lower than that of graphite and ash-free coal. Moreover, the output power density (258 mW cm^{-2}) of the DC-SOFC with Ca-loaded wheat straw char is acceptable for an electrolyte-support SOFC, which is higher than that of the DC-SOFCs operated on graphite and ash-free coal. From an economic point of view, wheat straw char is much suitable for large-scale industrial production.

4. Conclusions

A direct carbon solid oxide fuel cell (DC-SOFC) can be operated on biochar derived from wheat straw. SEM and EDX characterization show that the wheat straw char is porous and composed of C, K, Mg, Cl, Fe and Ca elements. XRD analysis indicated that the minerals of the wheat straw char is mainly composed of KCl, and obvious peaks attributed to CaCO_3 can be found after loading 5% of Ca (weight percent) on the wheat straw char. Raman analysis demonstrates that considerable content of disorder carbon exists in the wheat straw char, which might benefit the carbon gasification reaction. To demonstrate the catalytic activity of Ca on the wheat straw char, a programmed-temperature gravimetric experiment is conducted on the pure wheat straw char and the Ca-loaded wheat straw char. The results show that the Ca catalyst has excellent catalytic effect to the carbon gasification reaction, and further enhances the output performance of the corresponding DC-SOFCs. The maximum power density of the DC-SOFC operated on the pure wheat straw char is 197 mW cm^{-2} at 800°C , and increases to 258 mW cm^{-2} when 5% of Ca (weight percent), as a catalyst of the Boudouard reaction, is

loaded on the wheat straw char. Compared to activated carbon, graphite and ash-free coal, the wheat straw char has obvious advantages of low-cost and high output performance. Therefore, it could be developed into a safe and cost effective distributed power generation system for generating electricity using local biomass such as wheat straw as energy source.

Acknowledgements

This work was supported by the National Science Foundation of China (NSFC, No. 21276097), the Special Funds of Guangdong Province Public Research and Ability Construction (No. 2014A010106008), Guangdong Innovative and Entrepreneurial Research Team Program (No. 2014ZT05N200), the Joint Funds of National Science Foundation of China and Guangdong Province (NSFC-Guangdong, No. U1601207), and a fund from Environmental Conservation Fund of Hong Kong SAR (ECF 54/2015).

References

1. Shafiee S, Topal E. When will fossil fuel reserves be diminished. *Energy Policy* 2009; **37**(1):181-9.
2. Caputo AC, Palumbo M, Pelagagge PM, Scacchia F. Economics of biomass energy utilization in combustion and gasification plants: effects of logistic variables. *Biomass & Bioenergy* 2005; **28**(1):35-51.
3. Del Río JC, Prinsen P, Gutiérrez A. A Comprehensive Characterization of Lipids in Wheat Straw. *Journal of Agricultural and Food Chemistry* 2013; **61**(8):1904-13.

4. Wu CZ, Huang H, Zheng SP, Yin XL. An economic analysis of biomass gasification and power generation in China. *Bioresource Technology* 2002; **83**(1):65-70.
5. Al-Shemmeri TT, Yedla R, Wardle D. Thermal characteristics of various biomass fuels in a small-scale biomass combustor. *Applied Thermal Engineering* 2015; **85**:243-51.
6. Li X, Wang S, Duan L, Hao J, Li C, Chen Y, et al. Particulate and Trace Gas Emissions from Open Burning of Wheat Straw and Corn Stover in China. *Environmental Science & Technology* 2007; **41**(17):6052-8.
7. Xu H, Chen B, Liu J, Ni M. Modeling of direct carbon solid oxide fuel cell for CO and electricity cogeneration. *Applied Energy* 2016; **178**:353-62.
8. Xu H, Chen B, Zhang H, Sun Q, Yang G, Ni M. Modeling of direct carbon solid oxide fuel cells with H₂O and CO₂ as gasification agents. *International Journal of Hydrogen Energy* 2017; **42**(23):15641-51.
9. Cao T, Wang H, Shi Y, Cai N. Direct carbon fuel conversion in a liquid antimony anode solid oxide fuel cell. *Fuel* 2014; **135**:223-7.
10. Molino A, Giordano G, Motola V, Fiorenza G, Nanna F, Braccio G. Electricity production by biomass steam gasification using a high efficiency technology and low environmental impact. *Fuel* 2013; **103**:179-92.
11. Zhang H, Chen L, Zhang J, Chen J. Performance analysis of a direct carbon fuel cell with molten carbonate electrolyte. *Energy* 2014; **68**(68):292-300.
12. Rady AC, Giddey S, Badwal SPS, Ladewig BP, Bhattacharya S. Review of Fuels

- for Direct Carbon Fuel Cells. *Energy Fuel* 2012; **26**(3):1471-88.
13. Xu H, Chen B, Zhang H, Kong W, Liang B, Ni M. The thermal effect in direct carbon solid oxide fuel cells. *Applied Thermal Engineering* 2017; **118**:652-62.
 14. Jiao Y, Zhao J, An W, Zhang L, Sha Y, Yang G, et al. Structurally modified coal char as a fuel for solid oxide-based carbon fuel cells with improved performance. *Journal of Power Sources* 2015; **288**:106-14.
 15. Yang B, Ran R, Zhong Y, Su C, Tadé MO, Shao Z. A carbon–air battery for high power generation. *Angewandte Chemie International Edition* 2015; **54**(12):3722-5.
 16. Nakagawa N, Ishida M. Performance of an internal direct-oxidation carbon fuel cell and its evaluation by graphic exergy analysis. *Industrial & Engineering Chemistry Research* 1988; **27**(7):1181-5.
 17. Xie Y, Tang Y, Liu J. A verification of the reaction mechanism of direct carbon solid oxide fuel cells. *Journal of Solid State Electrochemistry* 2013; **17**(1):121-7.
 18. Cai W, Zhou Q, Xie Y, Liu J, Long G, Cheng S, et al. A direct carbon solid oxide fuel cell operated on a plant derived biofuel with natural catalyst. *Applied Energy* 2016; **179**:1232-41.
 19. Cai W, Liu J, Xie Y, Xiao J, Liu M. An investigation on the kinetics of direct carbon solid oxide fuel cells. *Journal of Solid State Electrochemistry* 2016; **20**(8):2207-16.
 20. Cai W, Zhou Q, Xie Y, Liu J. A facile method of preparing Fe-loaded activated carbon fuel for direct carbon solid oxide fuel cells. *Fuel* 2015; **159**:887-93.
 21. Tang Y, Liu J. Effect of anode and Boudouard reaction catalysts on the performance

- of direct carbon solid oxide fuel cells. *International Journal of Hydrogen Energy* 2010; **35**(20):11188-93.
22. Bai Y, Liu Y, Tang Y, Xie Y, Liu J. Direct carbon solid oxide Fuel Cell—a potential high performance battery. *International Journal of Hydrogen Energy* 2011; **36**(15):9189-94.
23. Elleuch A, Boussetta A, Yu J, Halouani K, Li Y. Experimental investigation of direct carbon fuel cell fueled by almond shell biochar: Part I. Physico-chemical characterization of the biochar fuel and cell performance examination. *International Journal of Hydrogen Energy* 2013; **38**(36):16590-604.
24. Zhou Q, Cai W, Zhang Y, Liu J, Yuan L, Yu F, et al. Electricity generation from corn cob char through a direct carbon solid oxide fuel cell. *Biomass & Bioenergy* 2016; **91**:250-8.
25. Corigliano O, Fragiaco P. Numerical modeling of an indirect internal CO₂ reforming solid oxide fuel cell energy system fed by biogas. *Fuel* 2017; **196**:352-61.
26. Qin H, Zhu Z, Liu Q, Jing Y, Raza R, Imran S, et al. Direct biofuel low-temperature solid oxide fuel cells. *Energy & Environmental Science* 2011; **4**(4):1273-6.
27. Cai W, Liu J, Yu F, Zhou Q, Zhang Y, Wang X, et al. A high performance direct carbon solid oxide fuel cell fueled by Ca-loaded activated carbon. *International Journal of Hydrogen Energy* 2017; **42**(33):21167-76.
28. Lei L, Bai Y, Liu J. Ni-based anode-supported Al₂O₃-doped-Y₂O₃-stabilized ZrO₂

- thin electrolyte solid oxide fuel cells with Y₂O₃-stabilized ZrO₂ buffer layer. *Journal of Power Sources* 2014; **248**:1312-9.
29. Lobo LS, Carabineiro SAC. Kinetics and mechanism of catalytic carbon gasification. *Fuel* 2016; **183**:457-69.
 30. Huang Y, Yin X, Wu C, Wang C, Xie J, Zhou Z, et al. Effects of metal catalysts on CO₂ gasification reactivity of biomass char. *Biotechnology Advances* 2009; **27**(5):568-72.
 31. Lahijani P, Zainal ZA, Mohamed AR, Mohammadi M. CO₂ gasification reactivity of biomass char: catalytic influence of alkali, alkaline earth and transition metal salts. *Bioresource Technology* 2013; **144**(3):288-95.
 32. Cazorla-Amorós D, Linares-Solano A, Lecea CS-Md, Joly JP. Calcium-carbon interaction study: Its importance in the carbon-gas reactions. *Carbon* 1991; **29**(3):361-9.
 33. Tomita A. Catalysis of Carbon–Gas Reactions. *Catalysis Surveys from Japan* 2001; **5**(1):17-24.
 34. Linares-Solano A, Almela-Alarcón M, Lecea SMD. CO₂ chemisorption to characterize calcium catalysts in carbon gasification reactions. *Journal of Catalysis* 1990; **125**(2):401-10.
 35. Irfan MF, Usman MR, Kusakabe K. Coal gasification in CO₂ atmosphere and its kinetics since 1948: A brief review. *Energy* 2011; **36**(1):12-40.
 36. Taylor HS, Neville HA. Catalysis in the interaction of carbon with steam and with

carbon dioxide. *Journal of the American Chemical Society* 1921; **43**:2055-71.

37. Dudek M, Tomczyk P, Socha R, Hamaguchi M. Use of ash-free “Hyper-coal” as a fuel for a direct carbon fuel cell with solid oxide electrolyte. *International Journal of Hydrogen Energy* 2014; **39**(23):12386-94.

Figure captions

Figure 1. Schematic illustration of a direct carbon solid oxide fuel cell.

Figure 2. SEM pictures of anode (a) and electrolyte (b) of the as prepared SOFC.

Figure 3. Output performances (a) and impedance spectra (b) of the as-prepared SOFC operated on humidified hydrogen at 800 °C.

Figure 4. SEM micrographs (a, b) and EDX results (c) of wheat straw char.

Figure 5. X-ray diffraction spectra for pure wheat straw char and Ca-loaded wheat straw char.

Figure 6. Raman spectra of wheat straw and commercial graphite.

Figure 7. Carbon conversion of pure wheat straw char and Ca-loaded wheat straw

char under CO₂ atmosphere at 800 °C.

Figure 8. Output performances (a) and impedance spectra at OCV (b) of the DC-SOFCs operated at 800 °C, respectively with pure wheat straw char and Ca-loaded wheat char as fuel.

Figure 9. Discharging characteristics of DC-SOFCs respectively with 0.4 g pure wheat straw char and Ca-loaded wheat straw char, operated at constant current of 300 mA cm⁻², at 800 °C.

Figure 10. Microstructures of the Ca-loaded wheat straw char before (a) and after (b) cell discharging operation.